JCTC Journal of Chemical Theory and Computation

Environmental Effects on Glycophorin A Folding and Structure Examined through Molecular Simulations

Hirsh Nanda,[†] Jonathan N. Sachs,[§] Horia I. Petrache,[‡] and Thomas B. Woolf*[,†]

Department of Physiology, Johns Hopkins University School of Medicine, 725 N. Wolfe Street, Baltimore, Maryland 21205, Laboratory of Physical and Structural Biology, NICHD, National Institutes of Health, Bethesda, Maryland 20892, and Department of Molecular Biophysics and Biochemistry, Yale University, New Haven, Connecticut 06520

Received September 29, 2004

Abstract: The human erythrocyte sialoglycoprotein glycophorin A (GpA) has been used extensively in experiment and simulations as a model of transmembrane helix−dimer formation, emphasizing the critical role of specific residue−residue interactions between helices in dimer stability. While the tertiary dimer structure is modulated by the hydrophobic lipid bilayer environment, we show that interactions of GpA with ordered interfacial water are commensurate to intrahelical forces. The role of lipid−water interface in stabilizing transmembrane proteins is not yet understood; however, dramatic water reordering in the presence of the transmembrane domains is observed from simulations and is possibly measurable by experiment. Interfacial interactions including anisotropic interactions with the polar headgroups might favor parallel association of transmembrane helices. To quantify forces capable of disrupting the GpA dimer, we generate folding/unfolding intermediates by replacement of the lipid bilayer with water, eliminating not only the native hydrophobic environment but also the native interfacial water region. Dramatic changes in the secondary, helical structures occur, with a transition from i,i+4 α-helix to i,i+5 π-helix and concomitant perturbation of the tertiary structure. Enforcing the native α-helix secondary structure by soft dihedral restraints restores the native tertiary structure, in essence substituting for the lack of the lipid−water interface. We suggest that differentiation between interactions within the lipid bilayer, including interactions with lipid headgroups and interfacial water can enrich our understanding of the thermodynamic stability of transmembrane domains.

Introduction

Transmembrane proteins provide a unique challenge to a full molecular understanding of their structure and function.[1,2] A fundamental problem is obtaining structural information, even with the availability of modern experimental techniques such as high resolution X-ray diffraction and solid-state NMR spectroscopy. This handicap has given the community just a limited number of membrane proteins for in-depth analysis of structure and folding, compared to globular proteins. At the time of this writing there are approximately 400 entries in the PDB for membrane proteins and >25 000 entries for globular proteins. On the other hand, membrane protein folding motifs may be simpler than their water soluble counterparts.[3−6] The membrane spanning region of proteins are usually closely packed bundles of α-helices or β-barrels. Furthermore, from primary sequence data alone, α-helical regions can often be identified through hydropathy scales,[7] and reliable methods for predicting membrane protein

* Corresponding author phone: (410)614-2643; fax: (410)614-4436; e-mail: woolf@groucho.med.jhmi.edu.
[†] Johns Hopkins University School of Medicine.
[‡] National Institute of Health.
[§] Yale University.

10.1021/ct049928y CCC: $30.25
Published on Web 04/09/2005

topology have been recently developed.[8,9] This makes some aspects of structural prediction easier. However, protein interactions with the anisotropic, heterogeneous environment of the membrane bilayer continue to challenge our understanding of folding and function.[10,11]

The association of the glycophorin A (GpA) transmembrane region has been studied intently as a model for elucidating how proteins fold in a lipid membrane environment.[3,12−14] The GpA transmembrane region consists of a homodimer formed by two parallel α-helices of more than 18 residues each. The α-helices are formed by the apolar residue sequences T_{74}LIIFGVMAGVIGTILLI$_{91}$, that self-associate within a hydrophobic lipid environment. The question becomes what relative contributions do protein−protein interactions and lipid−protein interactions have in driving protein assembly? Consequently, what types of interactions with the lipid bilayer modulate GpA structure and function?

Much of the literature on transmembrane protein folding has focused on specific protein−protein interactions. In particular, early mutagenesis work on the GpA dimer identified the key residue sequence, LIxxGVxxGVxxT, as being responsible for dimer formation.[15,16] Based on these findings, a model of the dimer structure was proposed[17] and later validated by NMR spectroscopy.[18,19] With the structure of the GpA dimer solved, molecular modeling has revealed that close residue contacts, required for an overall attractive van der Waals interaction, were allowed by the small, compliant Gly residues at the helical interface.[20−22] It is now believed that, in general, the highly conserved GxxxG motif [4] allows the close packing of transmembrane helices in other proteins to occur.

Insights gained from the above studies are thought to be generalizable to other transmembrane proteins. However, in addition to the GxxxG motif mentioned above, other statistically relevant sequence motifs were identified,[4] some suggesting alternative mechanisms for helix−helix associations in membranes. In particular, while the glycophorin model emphasized the importance of van der Waals interactions, other proteins use polar side chains buried in the hydrophobic region of the bilayer to electrostatically drive the association of transmembrane helix domains.[23−26] These examples highlight that membrane associated proteins may utilize aspects of the lipid environment to promote folding and function.

A number of experimental studies have shown that features of the lipid bilayer environment such as thickness, fluidity, and chemical composition affect the folding and function of membrane proteins. For example, disparate cellular processes such as the rhodopsin photocycle[27,28] and alamethicin channel formation[29] have been shown to depend on the monolayer intrinsic curvature, a distinct property of lipid assemblies. Lipid chain length has been shown to have a crucial affect on gramicidin channel formation.[30,31] Studies on GpA have shown that the type of detergent micelle can affect monomer affinity by several orders of magnitude although the dimer structure itself is not altered.[14,32]

Lipid bilayers are not simple slabs of hydrophobic matter. A large section of the lipid bilayer, the interfacial region, is significantly more polar than the hydrocarbon core. We therefore should not restrict our attention to interactions just within the hydrophobic core but instead take into account possible interactions with the polar interface. The role of the bilayer interface and its interplay with the apolar environment of the membrane in stabilizing the GpA dimer and influencing parallel helix packing is a central concern of this paper.

The use of molecular dynamics to gain insight into the behavior and function of globular proteins is by now well established.[33] Furthermore, the importance of the solvation environment in properly capturing protein dynamics has been shown in several studies.[34] This powerful tool is also capable of giving insight into the complicated lipid bilayer environment.[22,35] Both ensemble averages and dynamic properties of the system are obtainable through this method. Because all forces are calculated at the atomic level it is, in principle, possible to parse out the most relevant interactions responsible for the process of interest. Recently, MD computations have been successfully applied to membrane proteins, including bacteriorhodopsin,[36] rhodopsin,[37] gramicidin,[38−40] OmpA,[35,41] KcsA,[42] and GpA.[22,43] The role of protein−lipid interactions has been the main aspect of these studies.

The central thrust of the current molecular dynamics calculations is to address the effects of the lipid−water interface environment on GpA transmembrane structure. In particular, how are interactions with the interface and lipid hydrocarbon mediated to stabilize the dimer? To this end, we first analyze simulations of the GpA dimer in a dimyristoylphosphatidylcholine (DMPC) membrane (Figure 1a), where protein structure has been validated by solid-state NMR measurements,[19] to investigate the interactions of GpA with the various regions within the bilayer, including interfacial water. We find that interfacial water, which differs markedly from bulk due to interactions with the lipid headgroups, is further modified by strong interactions with the transmembrane GpA dimer. In addition, because of the parallel orientation of the GpA dimer along the bilayer normal, interfacial dynamics on the two sides are distinct.

An important framework for understanding membrane protein assembly is the two-stage model introduced by Popot and Engelman,[44] in which stable α-helices first form within the lipid bilayer and then tertiary association forms the final structure. The process of helical insertion into bilayers and spontaneous dimer formation using simulations is still beyond current computational abilities. However much can be learned about the folding process from simulations of dimer disruption. The GpA dimer appears to be a particularly stable construct. As we have reported earlier, dimer structure is modulated by bilayers of different lipid types, in a manner consistent with hydrophobic matching concepts.[22] However this modulation does not involve significantly different structural intermediates. It has also been shown that dimer association probability is affected by micelles of different detergent type but not dimer structure itself.[14,32] Since GpA in its native environment is in permanent interaction with interfacial water as well as lipid hydrocarbon, a simple way to disrupt the dimer is removal of lipids and replacement with water throughout the simulation box.

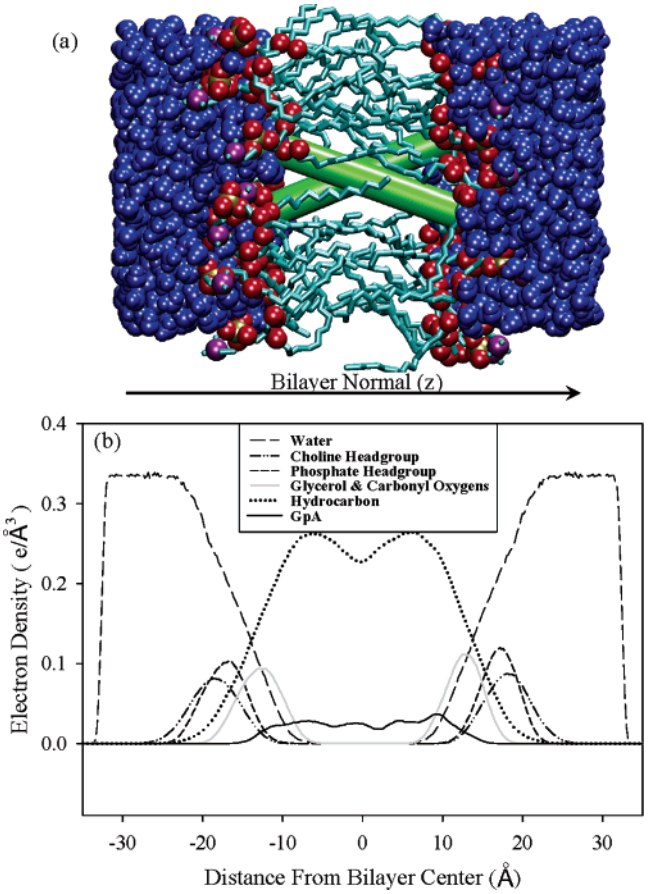

Figure 1. (a) Simulation snapshot of GpA in a DMPC bilayer. The protein is represented as cylinders (green), the lipid chains as lines (cyan), and the lipid headgroups and waters are shown as VdW spheres (water, blue; oxygen, red; phosphate, gold; nitrogen, violet). Hydrogens are omitted for clarity. (b) Electron density profile showing the distribution of molecular groups along the bilayer normal, averaged over the simulation.

By learning how the protein "falls apart" in the absence of the ordering potential of the membrane, we obtain insights into the role of the lipid/water interface in stabilizing the native protein structure. In addition, the water simulation allows us to quantify the asymmetry effect seen in the lipid simulation. Reassuringly, GpA structure is denaturated in water. Interestingly, however, the collapse of the tertiary and the secondary structure are very much interdependent. Indeed, by holding the backbone dihedral angles in the vicinity of the starting conformation (from NMR), we show that the tertiary structure is preserved, despite the absence of a native, bilayer environment to hold it in place. This suggests that, once helical monomeric structures are stabilized within both the hydrophobic core and the headgroup/water interface, dimer stability is assured.

Finally, allowing backbone dihedrals to evolve freely does not lead to direct unfolding into random coil conformations. Instead, exposure to water modulates backbone hydrogen bonding patterns, and alternate (metastable) dimer conformations are found throughout the length of the trajectory.

We suggest that interactions with the polar region of lipid bilayer, including direct and indirect perturbation of the interfacial water should be taken into account for molecular associations within transmembrane domains.

Materials and Methods

Bilayer Simulation Details. All bilayer simulations were performed using CHARMM versions 26 and 27[45] software and the CHARMM 27 parameter set. The DMPC pure bilayer system was constructed with 18 lipids per monolayer (36 lipids total), while the DMPC/GpA simulation was constructed with 45 lipids per monolayer (90 lipids total). Furthermore, 925 and 3756 waters were used in the pure DMPC and DMPC/GpA simulations, respectively, under the TIP3P water model. The construction of the membrane around the GpA molecule followed a procedure proposed by Woolf and Roux.[38,39] The NMR structure of GpA reported by MacKenzie et al.[18] was used as the initial structure for the GpA dimer.

Equilibration of both systems was performed initially through minimization and Langevin dynamics. The final set of equilibration and production was performed with a constant number of atoms (N), constant lateral surface area (A), constant normal pressure ($P = 1$ atm), and a constant temperature ($T = 298$ K) to give a NAP_NT ensemble. The total lateral surface area was 1075 Å^2 for the pure bilayer system and 3040 Å^2 for DMPC/GpA simulation. These values represent an area per lipid of 59.72 Å^2 that is consistent with experimental numbers[46] where for the DMPC/GpA system ~353 Å^2 was estimated for the dimer. All systems were run with periodic boundary conditions (PBC) using particle mesh Ewald for the treatment of long-range electrostatic interactions.[47] A cutoff of 12 Å was used for van der Waals interactions.[48] All bonds involving hydrogen atoms were fixed using the SHAKE algorithm[49] allowing a time step of 2 fs for dynamics. Lipid systems were simulated for a total of 1.5 ns and 22 ns for the DMPC and DMPC/GpA systems, respectively. The first 0.25 ns was taken as an equilibration period, and results are reported on the remaining simulation time. Further discussion involving ensemble choice and system construction can be found in ref 22.

GpA in Water Simulation Details. This set of simulations were performed using the CHARMM 27 software package with the CHARMM 27 parameter set. All simulations used periodic boundary conditions and particle mesh Ewald for long-range electrostatic interactions as well as a 12 Å cutoff for van der Waals interactions. Bonds to hydrogen atoms were fixed using the SHAKE algorithm allowing a 2 fs time step during dynamics.

The initial water box simulations used the same simulation conditions as the bilayer simulations. Namely, the NAP_NT ensemble was considered with a constant lateral area (A = 1200 Å^2), a constant normal pressure ($P_N = 1$ atm), and a constant temperature ($T = 298$ K). The simulation cell consisted of one GpA dimer molecule and 2060 waters. The system was constructed from an equilibrated water box with cell dimensions similar to those of the bilayer simulations. Waters that overlapped with the protein were deleted, and minimization was performed on the waters with all atoms of the protein fixed. This was then proceeded by 200 ps of

equilibration using constant normal pressure and constant temperature dynamics with the structure of the GpA dimer still fixed. The cell dimensions of the system were observed to have remained stable over the last 100 ps of equilibration. All restraints on the proteins were then removed, and two simulations were started each beginning with a different set of initial random velocities. The velocities were assigned using a Gaussian distribution such that the system was set to the proper temperature. These two GpA/water systems were then run out to the limit of available computational resources, 16 ns and 19 ns, respectively.

Construction of the large water boxes used an equilibrated, cubic, water box of larger dimensions with roughly double the volume of the bilayer simulations. Again the micelle structure of the GpA dimer was inserted into the system, and overlapping waters were deleted. This resulted in a system containing 5626 waters with cell dimensions of ~55.3 Å on each side. All three cell dimensions were allowed to vary under a constant pressure and temperature ensemble, *NPT*, with a pressure, $P = 1$ atm, and temperature, $T = 298$ K. The equilibration procedure was similar to that above; first all atoms of the GpA dimer were fixed, and then minimization on waters was performed followed by 200 ps of dynamics on the entire system. All restraints on the protein were then released, and three simulations were begun each starting with a different set of initial velocities. One simulation was run out for 5 ns of production. For the next two simulations a harmonic restraint was put on the dihedral angles of the backbone, and the systems were simulated for 2 ns each. The total 4 ns of simulation time was analyzed and reported in the results.

Hydrogen Bonding. There is no explicit hydrogen bonding term in the CHARMM 27 force field. For this reason backbone hydrogen bonding partners were identified by geometrical criteria. All hydrogens that were within a 90° angle cone of the hydrogen bond acceptor, carbonyl oxygen, and within 2.5 Å of the oxygen were considered potential hydrogen bonding partners. If more than one hydrogen satisfied the above criteria, they were further discriminated against using a smaller 135° angle cone and then considering the hydrogen with the shortest distance to the acceptor atom. The same algorithm was applied to finding water oxygen partners for the backbone amide hydrogen.

Results

The Native Lipid/Water Interface. There are distinct structural features along the bilayer normal of a membrane. Electron density profiles from a DMPC/GpA simulation in Figure 1b show the distribution of different molecular groups along this normal with the distributions weighted by the number of electrons for each molecular group. The membrane interface, defined as the region of the polar headgroups (phosphate and choline as well as the polar glycerol backbone and carbonyl oxygen), contributes to almost one-half of the bilayer thickness. Furthermore, there is a significant population of waters in this region. Some waters penetrate to within 10 Å of the bilayer center, well within the hydrocarbon region of the membrane and in contact with GpA.

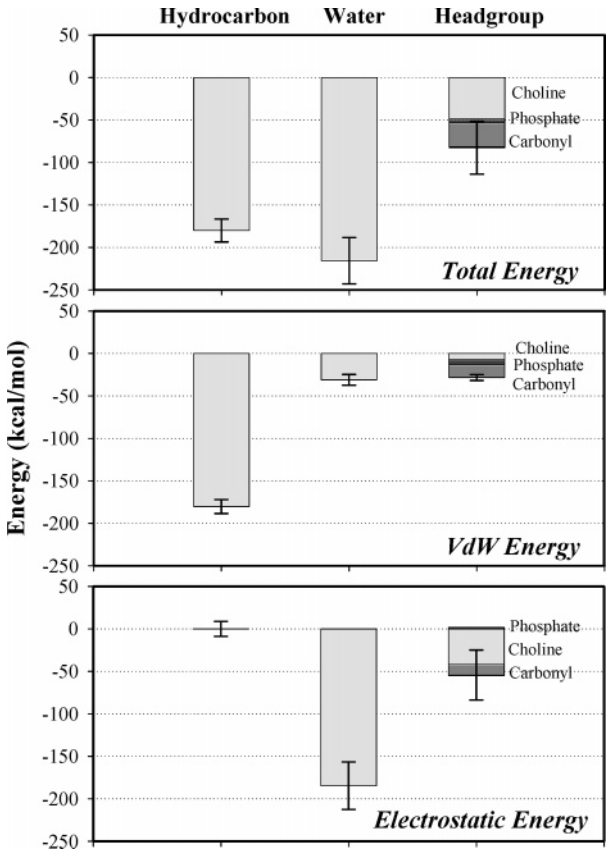

Figure 2. Average GpA interaction energy with bilayer environment in DMPC/GpA simulation. Interaction energy is decomposed into contributions from hydrocarbon, water, and headgroup. The headgroup term is further decomposed into phosphate, choline, and carbonyl\ester interactions. Mean square fluctuations are shown with error bars.

Figure 2a shows average interaction energies between the GpA dimer and the various polar and nonpolar groups of the lipid bilayer. It is striking that the protein−water interactions are the strongest. Interactions with the lipid hydrocarbon are also large, as expected, and are of roughly the same magnitude as water interactions. The combined contribution of the phosphate, choline, and glycerol/carbonyl groups (headgroup interactions) represent roughly 1/6 of the total interaction energy between the protein and its environment. However, if one considers the total membrane interface as the sum of the water and headgroup contributions, then interactions with the interface dominate over that of the lipid hydrocarbon. The interaction of individual helices with the lipid environment are statistically equivalent and half that of the total dimer interaction. Major differences in the breakdown into van der Waals and electrostatic components are also seen in Figure 2. As expected, the nonpolar lipid tails interact primarily through van der Waals interactions (Figure 2b), whereas the water interactions are electrostatically dominated (Figure 2c). The phosphate group has, on average, a small slightly repulsive electrostatic interaction with GpA, with large positive and negative fluctuations about the mean.

The strong interaction between the protein and water motivates a more detailed analysis of water behavior in the vicinity of the GpA dimer. Figure 3 compares water order

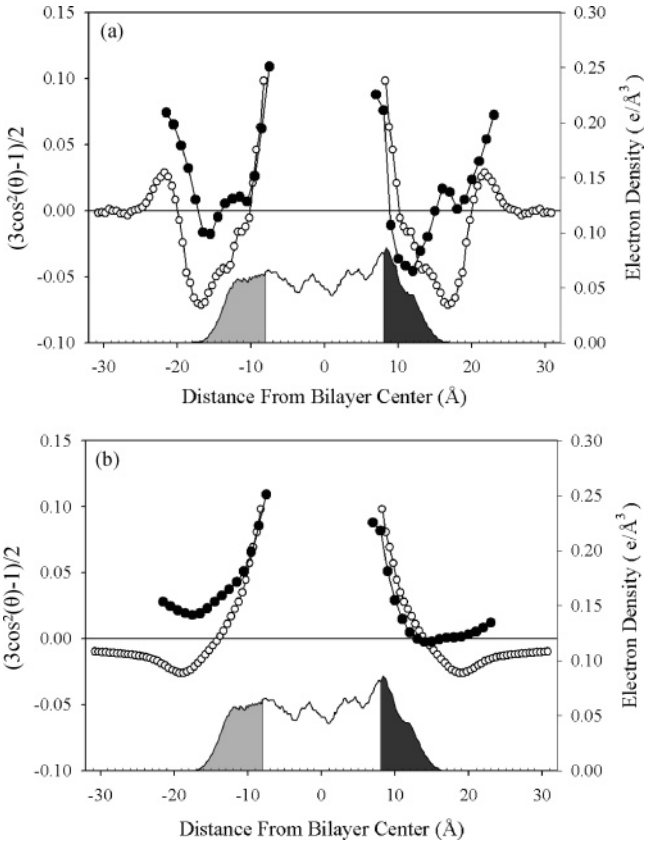

Figure 3. (a) Local second rank order parameters of water O−H bond orientation with respect to the membrane normal for simulations of pure DMPC (open circles) and DMPC/GpA (filled circles). For DMPC/GpA only water within a 6 Å radius of the protein was considered to emphasize the effect in the protein vicinity. GpA electron density profie is replotted from Figure 1b. The N-terminus amide hydrogen and the C-terminus carbonyl oxygen regions are shaded in light and dark gray, respectively. (b) Running averages (integrated profiles) of data in part (a).

parameters relative to the membrane normal with and without the GpA dimer. The average second-order Legendre polynomial, $(3\cos^2(\theta)-1)/2$, is plotted where θ is the angle of the O−H bond vector with the membrane normal. These second rank order parameters of the water O−H bonds are measurable by solid-state ^{2}H NMR in heavy water.[50] The NMR observable corresponds to running averages of these profiles as seen in Figure 3b. However, from simulations, local order parameters can be determined and are amenable to a more straightforward interpretation, Figure 3a. As shown by Figure 3, for a pure bilayer, interfacial water is ordered.[51−54] Away from the interface, water molecules have no preferred orientation (zero local order parameter), defining the bulk water region. As one moves into the membrane and the lipid headgroup environment, regions of the second rank order parameter with different signs are observed.[51−54] The parallel orientation of GpA causes significant alternation of water ordering, than that characteristic to lipid bilayers,[55] as shown by calculations within a 6 Å radius of the protein dimer (Figure 3). This includes the first two hydration shells of water around the protein as determined by radial distribution functions.[56] Furthermore, the parallel packing of the GpA homodimer introduces an asymmetry about the bilayer midplane, manifested through differences in water orientation at the two sides of the bilayer. There is a clear shift in water ordering at the N-terminus (negative z), when compared to ordering at the C-terminus (positive z). A possible interpretation is a tendency for water at the N-terminus to orient with the OH bond vector pointing away from the bilayer center. In contrast, at the C-terminus, water ordering is biased toward the bilayer center. The structural difference between the N- and C-termini of the GpA dimer is, obviously, the free amide hydrogens on one side and the carbonyl oxygens on the other. For reference to water order parameter profiles, these regions are highlighted in Figure 3.

Lipid Replacement. We now investigate the effect of removing the lipid molecules by filling the whole simulation box with water. This replacement not only eliminates the native hydrophobic environment of the GpA core but also destroys the water ordering characteristic of lipid/water interfaces (the native water environment of GpA). Because of these differences, major disruption of the GpA dimer is expected. However, despite radical structural changes, a helical secondary structure was still preserved in all water runs. Furthermore, the helices remained associated for the duration of the simulations. A comparison of the Cα root-mean-square deviation for the DMPC/GpA and water/GpA Run1 simulations show that initially there is a larger deviation in helix for the water run, Supplementary Figure 1 (see Supporting Information). However, as the protein stabilizes into the new helical structure the deviation plateaus. The nature of this hydrophobic association or aggregation in water will be described below. Without the shielding of the membrane, significant competition between intrahelical backbone hydrogen bonding and that with water occurs, as shown in Figure 4. GpA hydrogen bonding with water in the DMPC/GpA run is shown for comparison. In the bilayer setting, only the first four residues at the N-terminal side and the last four residues at the C-terminal side can hydrogen bond to water. The internal residues of the protein are shielded from water interactions by the lipid hydrocarbon region. The α-helices of the transmembrane dimer, stabilized by the i,i+4 intrahelical backbone hydrogen bonding motif, leaves the amide hydrogens of the first four residues at the N-terminus and the carbonyl oxygens of the last four residues at the C-terminus with unpaired donors and acceptors, respectively.

With the lipids replaced by water, increased hydrogen bonding between GpA and water is seen. Overall, there is a greater degree of water interactions with the backbone carbonyl oxygen. This is likely due to the ability of the water hydrogens to adopt favorable orientations while avoiding steric blocking from amino acid side chains. However, not all interior amino acids show the same degree of water hydrogen bonding. Reduced interactions with water are found for the residues at the helix−helix interface, in particular Gly79, Ala82, and Gly83. Other residues, Val80, Val84, and Ile85 exhibit minimal hydrogen bonding to water even though they are not involved in the helix−helix interface. These residues all contain β-branched side chains that can sterically block access to the protein backbone.

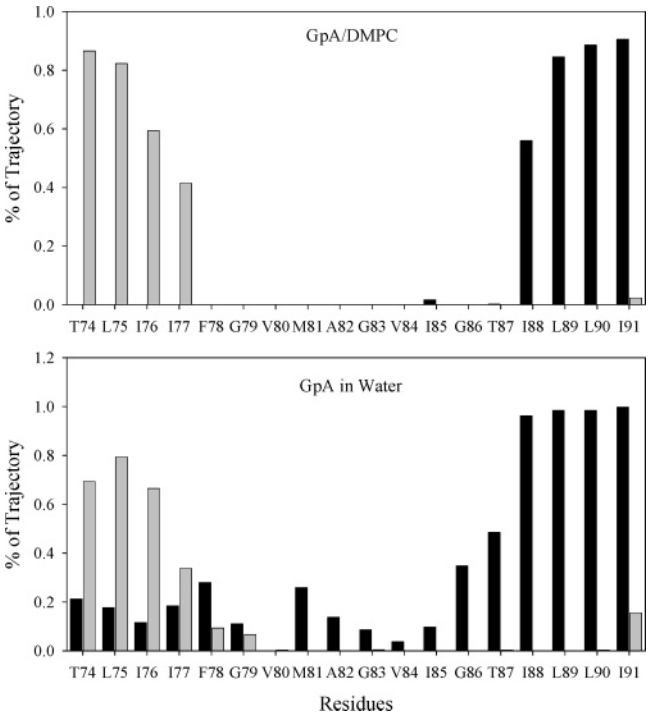

Figure 4. Fraction of simulation each residue spends forming backbone-water hydrogen bonds. Amide hydrogens to water bonds are shown in light gray; carbonyl oxygens to water bonds are shown in dark gray.

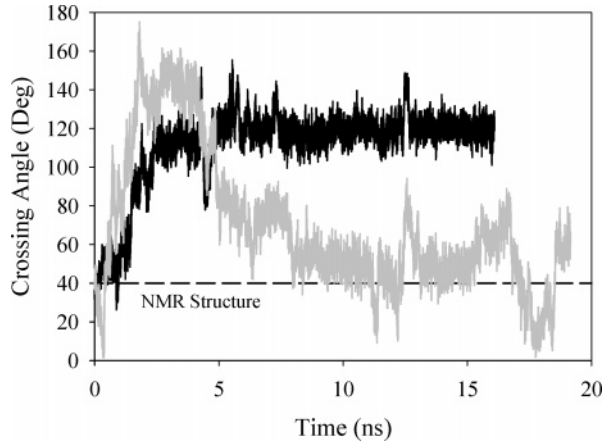

Figure 5. Time series of crossing angles for unconstrained water simulations, run1 (black) and run2 (grey). The experimental reference value[7] is indicated by the dashed line.

Despite preservation of a helical structure and dimer association, significant changes to secondary and tertiary structural elements were found in the water/GpA systems. The crossing angle between the two helices that make up the GpA dimer is a relevant parameter defining the tertiary structure of the protein. This angle is mediated by the interplay between interhelical interactions and interactions with the environment. Variations of this angle can be regarded as modifications of the net torque about the dimer crossing point. The time series of the helix crossing angle for the different simulations is plotted in Figure 5. As determined experimentally for GpA structures in micelles,[18] the GpA dimer has a crossing angle of about 40°. Analysis of the lipid simulation shows that the dimer structure differs only slightly within a DMPC bilayer, with a mean crossing angle of 44°. For the water simulations shown in Figure 5, significant deviations from these values are seen. Initially, within the first 2 ns of the simulation, both trajectories deviate rapidly and in a similar fashion from the NMR structure. At 2 ns, however, trajectories begin to diverge. One run stabilizes at a mean crossing angle of 120° for the duration of the simulation, ~12 ns. The helices in the second run, however, continue to rotate about each other, settling only slightly preferentially at approximately 50°. These water simulations were performed at the same system size as the lipid simulation for direct comparison of interaction energies. Simulation in an aqueous solution of a larger size showed similar trends, though changes occurred more slowly, implying that the smaller system dimensions do not inhibit further denaturation of GpA structure by water.

To further characterize the behavior of the GpA dimer in water, we recorded the intermonomer distance (between helical mass centers) and the length per residue for each helix. Compared to the DMPC/GpA simulation, the average center of mass distance in water increases by 1.5 Å. A decrease in the pitch per residue is also seen, to a value of 1.2 Å, compared to the α-helical 1.5 Å[57] found in DMPC. Interestingly, the pitch value that we find in water corresponds to a π-helix geometry. For a π-helix an increase in the helical radius of 0.5 Å is also expected.[57] This would result in at least a 1 Å increase in the center of mass distance between two packed helices, as we find in our simulations (also see above).

Constrained Secondary Structure. To study the interdependence of secondary and tertiary structures, we carried out simulations with the GpA backbone dihedral angles constrained by harmonic potentials in the vicinity of the NMR starting structures. The internally restricted GpA helices are otherwise free to move in space, in response to the denaturing, all-water environment. Under these conditions, we find an even more tightly packed dimer, with a center of mass between the two helices 0.7 Å less than in the DMPC bilayer. The most striking result is that the helix crossing angle remains roughly unchanged (stable at about 40°). Hence, preserving the secondary, α-helical structure resulted in conservation of the tertiary structure.

Is water ordering next to GpA also observed? We investigate this by comparison of the water dipole angle next to the dimer for the DMPC/GpA and constrained-backbone systems. Because in the pure water simulation there is no such reference frame as the bilayer normal, dipole angles are computed with respect to the helical axis for both the lipid and the water simulations. This calculation was performed within a cylinder with a 6 Å radius centered around the helix. The cylinder is extended beyond the ends of the helix into the bulk region of the system. For waters included in this cylinder, average water dipole orientations were calculated as a function of distance from the geometrical center of the helix, placed at zero (similar to the analysis in Figure 3).

Results are plotted in Figure 6. For the DMPC/GpA run, the water dipole orients away from the helix center initially. Further in, the orientation changes and the water dipole

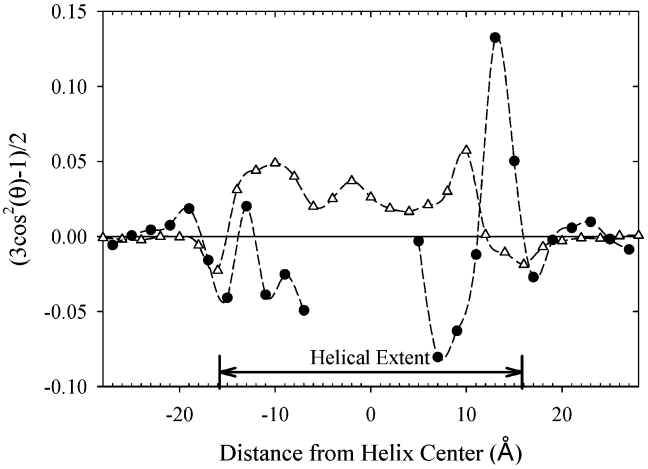

Figure 6. Water dipole order parameters with respect to the GpA monomeric axis for DMPC/GpA (filled circles) and constrained-backbone water/GpA (open triangles), averaged over both GpA helices. The helical extent is indicated at the bottom of the figure.

orients into the center. This behavior is similar to water orientation (measured by the OH bond vector) with respect to the membrane normal for a pure DMPC bilayer, Figure 3a. The bilayer strongly influences water orientation, and this is enhanced by the slight angle between the GpA helix axis and the membrane normal (<20°). From the constrained-backbone simulations, ordering of waters along the helix axis due solely to the protein (unbiased by the lipid environment) can also be observed. However, in the absence of the surrounding lipids, water ordering appears weaker and, interestingly, more symmetric than in the bilayer.

Comparison to NMR Measurements. Structural information on the membrane spanning region of GpA has come from both solution and solid-state NMR.[18,19] A set of 20 structures was determined (PDB code 1AFO) from NMR measurements in dodecylphosphocholine micelles. These structures were solved using a set of interhelical H−H NOE distance restraints along with J-coupling values sensitive to dihedral angles. Calculating the average interhelical H:H distances for the family of NMR structures and our simulations of GpA in a DMPC bilayer and GpA in water with a constrained-backbone gives us a basis for comparison to experiment. The hydrogen pairs considered correspond to those for which NOE distance restraints were assigned. For chemically equivalent hydrogens, the contribution of each hydrogen to the distance average was weighted by a factor of $1/r^6$. This is proportional to the drop off in NOE signal with respect to the distance, r. The results of these calculations can be seen in Figure 7a. There is generally good agreement between both the DMPC/GpA and constrained-backbone simulations with that of the NMR structure. However both simulations show a larger separation between hydrogens at the N-terminus and a greater mean square fluctuation at the C-terminus when compared to the NMR structures.

Further structural information has come from rotational resonance solid-state NMR of GpA in a DMPC bilayer.[19] This measurement gives a set of distance restraints between isotopically labeled carbons, shown in Figure 7b. While a

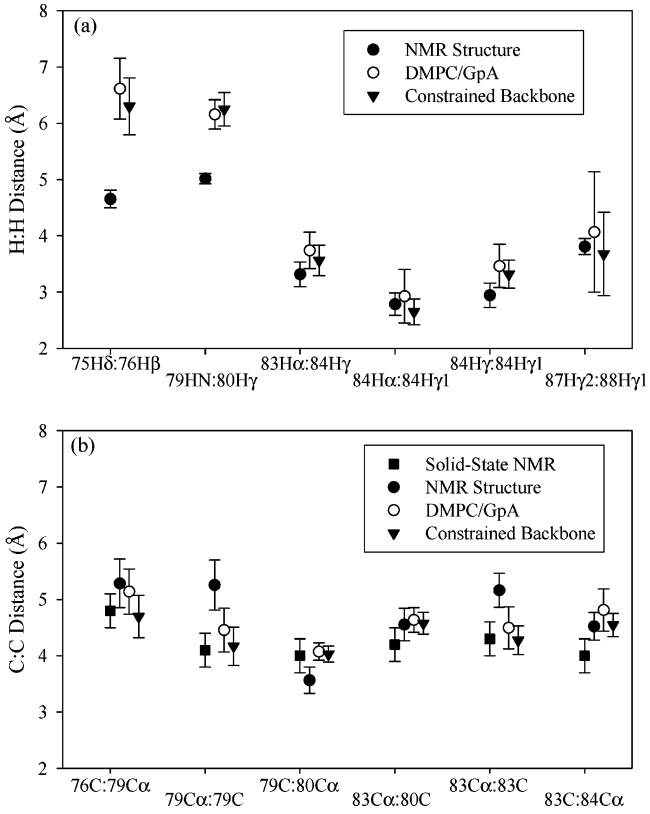

Figure 7. Comparison of simulations with NMR structural data. (a) Average interhelical H−H distances, corresponding to assigned NOE signals from solution NMR measurements.[7] Averages over 20 NMR structures (PDB code 1AFO) are shown with solid circles, DMPC/GpA simulation with open circles, and the constrained-backbone simulation with solid triangles. (b) Average interhelical C−C distances corresponding to solid-state NMR measurements (solid squares),[19] compared to the structures in part (a). Error bars represent mean square fluctuations.

formal protein structure was not solved, these average C−C distances can be compared between the various simulations and experiments. We find similar C−C distances between the bilayer simulation, the constrained-backbone water simulation, the solution NMR structure, and the solid-state NMR measurements. There appear to be subtle differences in C−C distances between the structure from the micelle and from the bilayer measurements. Both simulations analyzed here are in good agreement with the experimental data. The striking agreement between the constrained-backbone simulations and both the solution and solid-state NMR data emphasizes that the preservation of secondary structure results in preservation of tertiary packing between the two monomers.

Intermonomer Side-Chain Interactions. A detailed picture of how the environment affects interhelical interactions can be seen through residue−residue interaction energy matrices shown in Figure 8. In these plots, darker squares represent favorable or attractive residue interactions, and lighter squares represent unfavorable or repulsive residue interactions. Representative snapshots of the dimer structure for each system are also shown. The plot for the GpA simulation in DMPC and the constrained backbone simula-

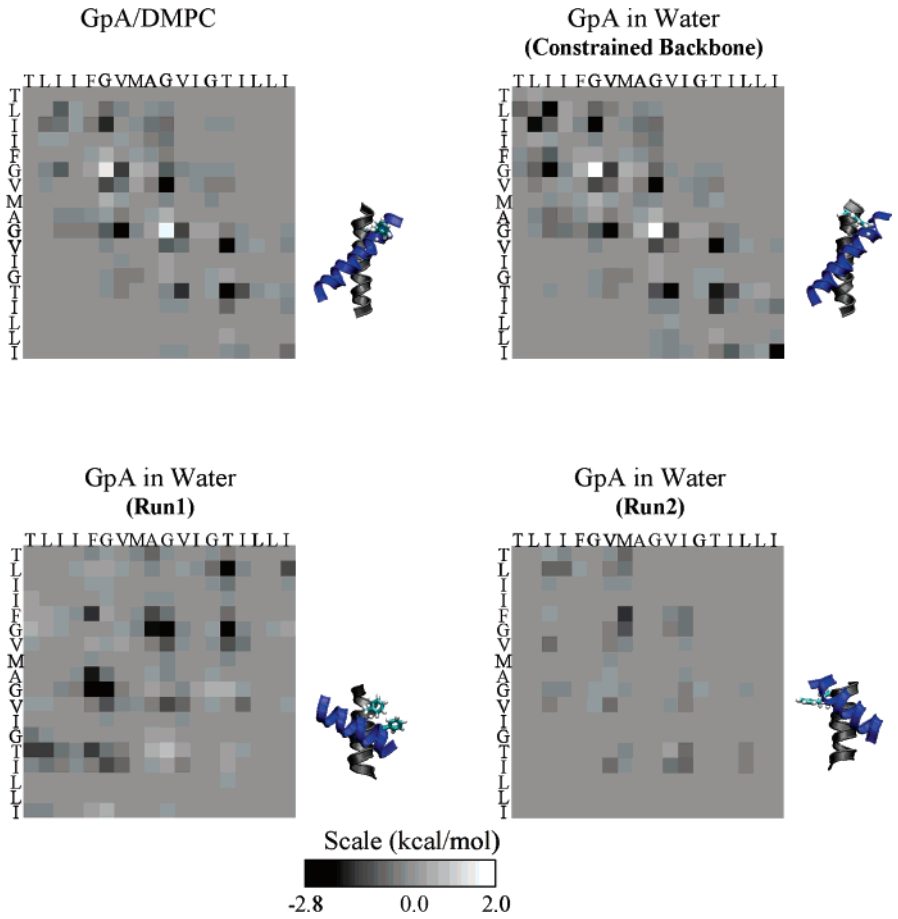

Figure 8. Average residue−residue interaction energy maps between GpA helices and representative snapshots from the simulations. Dark squares are favorable residue interactions and light squares are unfavorable residue interactions. Water/GpA Run1 is an average over the last 7 ns of the simulation. Water/GpA Run2 is an average taken from the 8−15 ns interval of the simulation.

tion in water (Figure 8, top panels) show the primary residues involved in the helix−helix interface to be consistent with the $L_{75}I_{76}xxG_{79}V_{80}xxG_{83}V_{84}xxT_{87}$ motif determined through numerous mutagenesis and structural studies.[15−17] The two glycines in the highly conserved GxxxG motif have a slightly unfavorable interresidue interaction with the corresponding glycines of the other helix. As we have shown previously for GpA in simulations of several different lipid types,[22] the repulsive Gly−Gly interaction is an electrostatic one, originating from the two closely packed backbone carbonyls and the two $C_\alpha H_2$ groups, from each helix glycine. The residue−residue interaction energy map of the constrained-backbone simulation is very similar to the bilayer simulation. Furthermore, interhelical backbone hydrogen bonding interactions between C_α-H···O═C groups of Gly79-Ile76, Val80-Gly79, and Gly83-Val80 appear to be conserved. This is consistent with the crossing angle result above, suggesting that native helix−helix packing interactions are conserved once native helical structures are preserved.

Analysis of free GpA in water (backbone restraints removed), for which π-helices are observed, presents markedly different interaction matrices (Figure 8, bottom panels). In one case, residue−residue interactions occur along the other diagonal of the matrix, indicative of an antiparallel helix packing motif. This is consistent with the 120° crossing angle reported above and shown by the representative snapshot in Figure 8. This alternate crossing angle of the GpA dimer appears to also be stabilized by a specific residue−residue interaction energy pattern. In the second case, corresponding to large fluctuations in the crossing angle (Figure 5), the interaction map resembles the upper panels, but the residue motif is less pronounced. The interactions are overall weaker, due to the fact that the center of mass distance between the helices is greater (see above). Here we show interaction energies averaged over the 8 to 15 ns time interval where the dimer crossing angle appeared most stable. Finally, the highlighted Phe groups in the snapshot serve as a dial showing that slightly different helical faces are in contact compared to the bilayer conformation

Backbone Structures. The distortion of the α-helical secondary structure observed in the water/GpA simulations implies a change in the intrahelical backbone hydrogen bonding motif. We looked at the time series of the backbone hydrogen bonding behavior with the total number of backbone hydrogen bonds divided into several categories. (1) The 3/10 helix i,i+3 motif, (2) α-helix, i,i+4 motif, (3) the π-helix, i,i+5 motif, and (4) water hydrogen bonding. The percent of all the GpA dimer backbone hydrogen bonds in each of these five categories was calculated as a function of time and plotted in Figure 9.

By design, the constrained-backbone simulation is not capable of significant secondary structural changes, so the

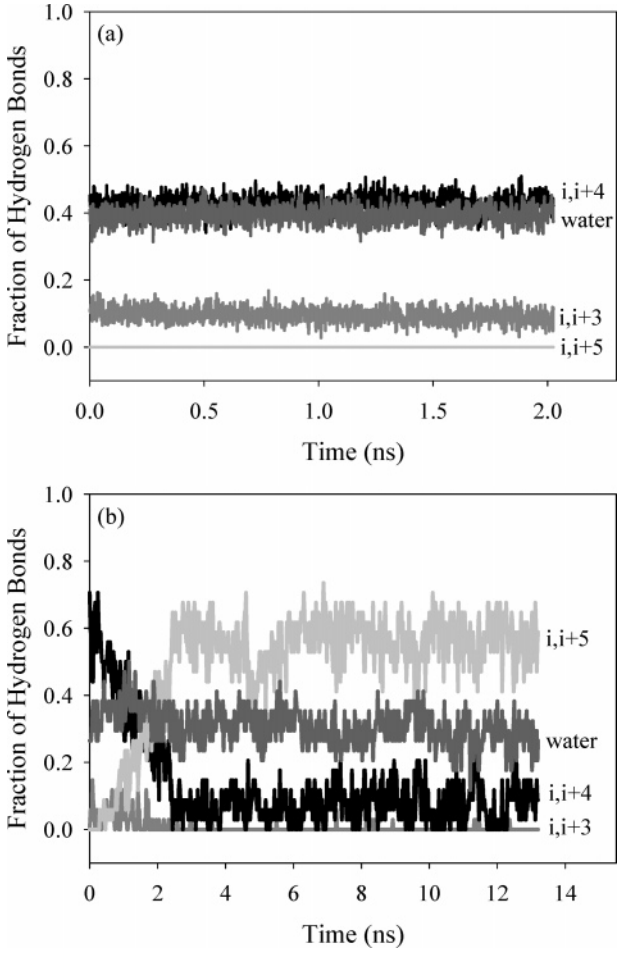

Figure 9. Time series of backbone hydrogen bonding patterns: (a) constrained backbone simulation and (b) water/GpA Run1 simulation.

time series of hydrogen bonding patterns in Figure 9a has a fairly constant behavior as given by the strength of the restraining potential. The α-helical, i,i+4, hydrogen bonding motif, and hydrogen bonding to water make up about 80% of all backbone hydrogen bonds. There is also a small degree of the 3/10 helix formation as well. Finally there is no indication of the π-helix associated hydrogen bonding pattern.

The behavior of the water/GpA Run1 is dramatically different (Figure 9b). Most noticeably, there is a rapid change within the first 3 ns, going from the i,i+4 hydrogen bonding motif to mostly i,i+5. The percentage of i,i+3 hydrogen bonding goes to zero. While fluctuations in hydrogen bonding patterns are greater for the water/GpA Run 1, the π-helix like conformation is stable throughout the majority of the trajectory. Furthermore from monitoring the time series of individual residue backbone hydrogen bonding, we find that Ala83-Gly84 and Ile86-Gly87 are the most common nucleation sites for π-helix formation (data not shown). Stabilization of a π-helix is found in both of the GpA in water simulations and represents a consistent affect of water on secondary structure.

The average backbone hydrogen bonding behavior of all simulations is given in Table 1. Averages for the free GpA dimer in water simulations were taken over the last 7 ns

Table 1. Fraction of GpA Backbone Hydrogen-Bonding Motifs Observed during Simulations[a]

system	i,i+3	i,i+4	i,i+5	water	other
constrained backbone	0.1	0.4	0	0.4	0.1
water/GpA (Run1)[b]	0	0.05	0.6	0.3	0.05
water/GpA (Run2)[b]	0	0.1	0.55	0.3	0.05
DMPC/GpA	0.05	0.7	0	0.2	0.05
DMPC/GpA (term res)	0	0.4	0	0.4	0.2

[a] Fluctuations about the mean were similar, in the range of ±0.02 to 0.05. [b] Average taken over the last 7 ns of the simulation.

Table 2. GpA Helix Interaction Energies in kcal/mol[a]

system	DMPC/ GpA	constrained backbone	water/ GpA (Run1)[b]	water/ GpA (Run2)[b]
electrostatic self-energy	−21.3	−13.7	−2.4	−3.4
environment interaction energy	−478.4 (−215.6)[c]	−490.6	−529.6	−554.3

[a] Errors about mean energy values were small and in the range of ±0.1 to 0.5 kcal/mol. [b] Average taken over last 7 ns of simulation. [c] Interaction with waters only.

where hydrogen bonding behavior appears to have stabilized. The constrained-backbone simulations show a much greater degree of hydrogen bonding with water than the simulation of DMPC/GpA. However if one just looks at the hydrogen bonding behavior of the 4 terminal residues at both the N- and C-terminus, the ratio of hydrogen bonding patterns are in better agreement. These terminal residues are significantly more exposed to water as was shown in Figures 1b and 4. Simulations of the free GpA molecule in water show similar behavior, with the i,i+5 helix conformation becoming strongly favored.

The shift in backbone structure corresponds to a change in the energetics of helix stability. This can be seen from the electrostatic self-energies of the protein helices in the different simulations (Table 2). GpA in the π-helix conformations have electrostatic self-energies nearly an order of magnitude less than in the α-helical structures in DMPC and the constrained-backbone simulations. Electrostatic self-energies are stronger in the bilayer environment. There is an inverse relationship between protein self-energy and GpA interaction with its environment, also shown in Table 2.

Discussion

Using GpA as a model system, the analysis described here begins to build a framework for the critical role of the bilayer interface in stabilizing membrane protein structure. We have shown that transmembrane domains interact strongly with the polar headgroup region of the lipid bilayer, possibly implicated in favoring a parallel helical orientation rather than antiparallel. This should not come as a surprise, based on accumulating evidence on bilayer structures, especially with regard to the spatial extent of the headgroup region (Figure 1b). The molecular distributions shown in Figure 1b are consistent with X-ray and neutron scattering as well as NMR spectroscopy.[22,58−62] While the folding of membrane proteins is primarily dictated by the hydrophobic environment at the bilayer center, the stability of its functional form can be influenced by interactions at the lipid/water interface.

We have also shown that the preservation of the secondary structure maintains the integrity of the tertiary structure even when the native lipid environment is (admittedly artificially) replaced by water. This suggests, although does not directly prove, that once helical structures are formed within the bilayer, dimer association is favored, consistent with the two-stage model of Popot and Engelman.[44] It is important to note that secondary structures were constrained internally through soft harmonic potentials on backbone dihedral angles only. These soft potentials did not prevent overall helical motions (translation or rotation), nor did they act on side-chain atoms. The strength of the constraining potential was such that distance fluctuations shown in Figure 7 were comparable in magnitude to experimental measurements in micelles and bilayers. The dependence of tertiary structure on the preservation of secondary structure is further seen when the constraints on the backbone are removed.

Full exposure of the free GpA dimer to an aqueous environment destabilizes both the native tertiary and the secondary structures. While this modification can be readily labeled "hydrophobic collapse", we see a surprising degree of order in the collapsed protein. On the time-scale of these simulations one cannot assume that the highly structured collapsed protein material is in a thermodynamically stable denatured state. However, it may be possible that the sampled structures represent meta-stable unfolding/folding intermediates. Because the dimer is driven to an alternative, structured configuration, simulations in water show how an aqueous environment disrupts the protein and indirectly suggest how the membrane environment holds it stable. The convenient structural parameters to evaluate the GpA dimer are the helix−helix crossing angle, the center of mass distance between the helices, and the length/residue of the helix. Following these indicators, we see that there are several paths to disruption of the tertiary dimer structure, but modification of secondary structure is consistent.

The phase space of the denatured state is large, and it is not surprising that the water/GpA Run1 and Run2 explore different crossing angles. The differences in the crossing angle are likely an indication that the helical association behaves more like nonspecific aggregation. This is expected because disruption of the helical secondary structure breaks the native packing surface between helices. Even when crossing angles in the water/GpA Run2 approach those of the GpA in DMPC there are no native contacts between the two helices as seen in residue−residue interactions of Figure 8.

A helix motif was clearly preserved in all simulations of the free protein in water, despite the disruption of the α-helix form. The pitch per residue of 1.2 Å that we obtain is characteristic of a π-helix conformation. The π-helix was first proposed as another theoretical construct of an energetically stable helix conformation in addition to the α-helix.[57] Rare occurrences of this helix in nature have been shown in globular proteins and proposed as transient structures in membrane proteins.[63] The π-helix structure is thought to be stabilized by an i,i+5 backbone hydrogen bonding pattern. This would allow for a more loosely wound helix than an α-helix which has an i,i+4 hydrogen bonding motif. Analysis shows an initial, rapid changing from i,i+4 α-helix motif to an i,i+5 motif on a time scale of 2−3 ns (Figure 9).

Nucleation of π-helix formation was predominantly found at the glycine residues. In globular proteins glycines are known to be helix breakers.[64] The absence of a side chain in glycine residues allows greater conformational flexibility to the protein backbone, although their affect on helicity is position dependent.[64] Despite the effect on water soluble α-helices, glycines are commonly found in membranes proteins.[4] Previous simulations of transmembrane proteins in an aqueous setting have also reported on the occurrence of π-helices. These include simulations of the alamethicin channel-forming peptide and a poly-alanine helix in water,[65,66] and transmembrane segments of bacteriorhodopsin, which were simulated using Langevin dynamics in a bulk medium of high dielectric.[67]

It is of interest to compare these results with previous experimental work on the stability of poly-Ala helices. Poly-Ala peptides do not form stable α-helices by themselves in aqueous solution. However, the introduction of polar and especially charged guest residues are able to stabilize water soluble monomer helices.[68,69] Stability is increased by the greater number of substitutions. This behavior has been attributed to the desolvation of the alanine backbone NH and CO groups due to the preferential hydration of the polar residues.[70] These hydration deprived residues form tighter intrahelical hydrogen bonds, driving α-helix formation. Parallels can be drawn to membrane proteins where the lipid hydrocarbon environment severely dehydrates the backbone of the transmembrane helix.

A framework for α-helix stabilization in membranes through compensation of electrostatic interactions and entropy is suggested. Simulations of poly-Ala in various dielectric mediums show that helix instability can be induced by raising the bulk dielectric constant of the media.[70] As mentioned previously, a direct α-helix to π-helix transition can be induced in bacteriorhodopsin helices by raising the dielectric of the bulk media.[67] A low dielectric medium would favor short, rigid hydrogen bonds of an α-helix, whereas a higher dielectric would favor longer bond lengths (such as a π-helix) in order to allow for greater conformational flexibility. The results presented here may provide a more detailed molecular picture of how an aqueous setting disrupts a transmembrane α-helix. In the polar aqueous solution, restrictions on hydrogen bonding are relaxed allowing for increased water hydrogen bonding interactions and increased backbone and side-chain flexibility. In contrast, the lipid hydrocarbon region appears to be important for suppressing fluctuations out of the native secondary structure of the protein. Namely, by increasing the energetic importance of backbone hydrogen bonding interactions, the α-helix conformation is stabilized. This then drives the association of the transmembrane helices, because the α-helix conformation presents an optimized, unique face that stabilizes interhelical association, mainly through van der Waals, specific residue−residue interactions.[18]

While the two-stage model gives an important framework for understanding transmembrane protein assembly, the role of the interface environment on protein structure, not just

helix association, remains to be addressed. As shown by the molecular distributions in Figure 1, about 1/5 of the peptide length lies within the headgroup region where it is exposed to water. Including the peptide open ends in the membrane plane, a total of 2/5 of GpA surface is exposed to water. A peptide with primarily apolar side chains still has an amphipathic quality due to its polar backbone. An α-helix, in particular, is capable of significant hydrogen bonding interactions with water because of the i,i+4 motif leaves four residues each at the N- and the C-termini with unsatisfied hydrogen bonds. Thus, water molecules on either side of the membrane can hydrogen bond to backbone amide hydrogens and to the carbonyl oxygen groups. This may explain why glycophorin interactions with water are shown to be predominantly electrostatic. Satisfying this hydrogen bond pairing is of particular importance to membrane proteins. The cost of burying an unpaired hydrogen bond into a hydrophobic region is thought to be extremely unfavorable, 1.5 kcal per hydrogen bond,[2] though this can vary with respect to the position within the bilayer. We see significant water hydrogen bonding for the first four and last four residues of each helix, even when penetration into the hydrocarbon region is required to do so. In the case of the glycophorin dimer, we find that interactions with interfacial water can easily dominate over other relevant terms.

These results also point out the need to recognize some assumptions in using the GpA transmembrane domain as a model system for understanding membrane protein assemblies in both the experimental and simulation literature. By studying only the transmembrane domain the protein is truncated at the bilayer interface, whereas the full membrane protein would extend into the aqueous environment on both sides of the bilayer. The artificial truncation of the protein results in free terminal groups with unpaired backbone hydrogen bonds and may increase interactions with water and the membrane interface. However the interfacial region is indeed very broad, and the extended (untruncated) protein would actually have an increased surface area exposed to the polar region of the membrane. In fact, charged residues are often found near the N- and C-termini of membrane spanning helix domains where they are thought to mediate hairpin turns.[71] The presence of charged residues such as Lys or Arg as well as aromatics such as Trp or Tyr would significantly influence a proteins interactions with the membrane environment in general and the polar headgroups more specifically. The GpA protein sequence studied lacks these types of residues and represents interactions with purely apolar side chain groups. However, the value of the GpA transmembrane domain as a model system has been shown through many insights gained from numerous experimental and simulation studies. Finally helices that naturally end in the membrane region may take advantage of water in the capping of terminal hydrogen bonds.

In discussing interfacial interactions, one recognizes that water in the membrane interface has very different behavior from bulk water. As shown in Figure 3, interaction with lipid headgroups induces water ordering, measurable by solid-state NMR[52,53] and Raman spectroscopy.[72] Relative to the *local* membrane surface, water order profiles alternate between oxygens mainly pointing out toward the aqueous phase and a reversal with water oxygens pointing in toward the bilayer center. On a larger scale, that allows for membrane shape fluctuation, such profiles are smoothed out, as detected by ^{2}H NMR.[50,73,74] Experimentally, water is found to be strongly perturbed at distances of about 5 Å from the bilayer surface, corresponding to 10−15 waters per lipid headgroup.[73,74] A similar number is obtained in our simulation from the order profiles. This water fraction is also seen in Figure 1; it corresponds to that part of the water density profile that drops below the plateau value. When lipid headgroups are displaced by GpA, this water hydrates peptide termini.[75]

Analogies between water ordering next to lipid membranes and at interfaces with nonpolar liquids, air, and even solid surfaces can be drawn from literature to lend some understanding to interfacial water properties.[76,77] Ordering is generated, or at least enhanced, by the fact that interfacial waters cannot satisfy all hydrogen bonding sites, as it does in isotropic bulk. On average, waters at interfaces have one unsatisfied hydrogen bond per molecule.[54,76] Compensation through stronger hydrogen bonding networks at the interfaces can occur, including bonding with other solute molecules present at the interface. With an α-helix presenting unpaired partners, water-backbone hydrogen bonding is energetically favored by both the solute (peptide) and the solvent (water).

In summary, an important role of the membrane interface in the folding of membrane proteins[2] is suggested by our simulations. Consistent with the two stage model, the polypeptide is thought to first fold into an α-helix while inserting into the membrane. Second, intermonomer association occurs once α-helical domains are stabilized by the hydrocarbon environment. Dimer formation appears to be driven by strong, specific residue−residue interactions (Figure 8). Furthermore, favorable packing interactions occur between the apolar side chains and the lipid chain.[2] The role of the lipid−water interface, however, in stabilizing or modulating membrane protein structure is not as well understood in this scheme. With regard to the dimer crossing-angle, it is striking that the native GpA dimer is parallel rather than antiparallel, as this arrangement breaks the symmetry about the center of the lipid bilayer. In particular, as we show in Figure 3, interfacial water is differentially perturbed at the C- and N-termini, hence the bilayer sides are qualitatively different. Why is the parallel configuration preferred in the bilayer setting? When the constraints imposed by the lipid bilayer are removed, the dimer crossing-angle may increase if not flip (Figure 5). The constrained backbone simulations in water suggest that strong and specific packing interactions dictate the crossing angle between helices. Furthermore, perhaps this asymmetry aspect should be viewed in its full three-dimensional setting. Viewed in the membrane plane, the GpA dimer has a antiparallel orientation, suggesting that the alteration of a lipid headgroup arrangement in the membrane plane may be worth addressing.

Acknowledgment. We thank Vikas Nanda and Alfonso Leyva for helpful discussions and critical reading of the manuscript. This research was supported in part by a grant

from the NIH (R01GM064746). J.N.S. was funded by the Whitaker Foundation for Biomedical Engineering.

Supporting Information Available: Cα root-mean-square deviation (RMSD) for DMPC/GpA simulation and water/GpA Run1 simulation (Supplementary Figure 1). This material is available free of charge via the Internet at http://pubs.acs.org.

References

(1) Popot, J. L.; Engelman, D. M. Helical membrane protein folding, stability, and evolution. *Annu. Rev. Biochem.* **2000**, *69*, 881−922.

(2) White, S. H.; Wimley, W. C. Membrane protein folding and stability: Physical principles. *Annu. Rev. Biophys. Biomol. Struct.* **1999**, *28*, 319−365.

(3) Russ, W. P.; Engelman, D. M. The GxxxG motif: A framework for transmembrane helix-helix association. *J. Mol. Biol.* **2000**, *296* (3), 911−919.

(4) Senes, A.; Gerstein, M.; Engelman, D. M. Statistical analysis of amino acid patterns in transmembrane helices: The GxxxG motif occurs frequently and in association with beta-branched residues at neighboring positions. *J. Mol. Biol.* **2000**, *296* (3), 921−936.

(5) Ubarretxena-Belandia, I.; Engelman, D. M. Helical membrane proteins: diversity of functions in the context of simple architecture. *Curr. Opin. Struct. Biol.* **2001**, *11* (3), 370−376.

(6) Curran, A. R.; Engelman, D. M. Sequence motifs, polar interactions and conformational changes in helical membrane proteins. *Curr. Opin. Struct. Biol.* **2003**, *13* (4), 412−417.

(7) Jayasinghe, S.; Hristova, K.; White, S. H. Energetics, stability, and prediction of transmembrane helices. *J. Mol. Biol.* **2001**, *312* (5), 927−934.

(8) Krogh, A.; Larsson, B.; von Heijne, G.; Sonnhammer, E. L. L. Predicting transmembrane protein topology with a hidden Markov model: Application to complete genomes. *J. Mol. Biol.* **2001**, *305* (3), 567−580.

(9) Melen, K.; Krogh, A.; von Heijne, G. Reliability measures for membrane protein topology prediction algorithms. *J. Mol. Biol.* **2003**, *327* (3), 735−744.

(10) Gouaux, E.; White, S. H. Membranes − Lipids lost, lipids regained − Editorial overview. *Curr. Opin. Struct. Biol.* **2001**, *11* (4), 393−396.

(11) Gouaux, E.; White, S. H. Membranes − Proteins and membranes − a fusion of new ideas − Editorial overview. *Curr. Opin. Struct. Biol.* **2003**, *13* (4), 401−403.

(12) Fleming, K. G.; Ackerman, A. L.; Engelman, D. M. The effect of point mutations on the free energy of transmembrane alpha-helix dimerization. *J. Mol. Biol.* **1997**, *272* (2), 266−275.

(13) Liu, W.; Crocker, E.; Siminovitch, D. J.; Smith, S. O. Role of side-chain conformational entropy in transmembrane helix dimerization of glycophorin A. *Biophys. J.* **2003**, *84* (2), 1263−1271.

(14) Fisher, L. E.; Engelman, D. M.; Sturgis, J. N. Effect of detergents on the association of the glycophorin A transmembrane helix. *Biophys. J.* **2003**, *85* (5), 3097−3105.

(15) Lemmon, M. A.; Flanagan, J. M.; Hunt, J. F.; Adair, B. D.; Bormann, B. J.; Dempsey, C. E.; Engelman, D. M. Glycophorin-a Dimerization Is Driven by Specific Interactions between Transmembrane Alpha-Helices. *J. Biol. Chem.* **1992**, *267* (11), 7683−7689.

(16) Lemmon, M. A.; Flanagan, J. M.; Treutlein, H. R.; Zhang, J.; Engelman, D. M. Sequence Specificity in the Dimerization of Transmembrane Alpha-Helices. *Biochemistry-Us* **1992**, *31* (51), 12719−12725.

(17) Treutlein, H. R.; Lemmon, M. A.; Engelman, D. M.; Brunger, A. T. The Glycophorin-a Transmembrane Domain Dimer − Sequence-Specific Propensity for a Right-Hanqded Supercoil of Helices. *Biochemistry-Us* **1992**, *31* (51), 12726−12733.

(18) MacKenzie, K. R.; Prestegard, J. H.; Engelman, D. M. A transmembrane helix dimer: Structure and implications. *Science* **1997**, *276* (5309), 131−133.

(19) Smith, S. O.; Song, D.; Shekar, S.; Groesbeek, M.; Ziliox, M.; Aimoto, S. Structure of the transmembrane dimer interface of glycophorin A in membrane bilayers. *Biochemistry-Us* **2001**, *40* (22), 6553−6558.

(20) Lemmon, M. A.; Engelman, D. M. Specificity and Promiscuity in Membrane Helix Interactions. *Febs. Lett.* **1994**, *346* (1), 17−20.

(21) Adams, P. D.; Engelman, D. M.; Brunger, A. T. Improved prediction for the structure of the dimeric transmembrane domain of glycophorin A obtained through global searching. *Proteins* **1996**, *26* (3), 257−261.

(22) Petrache, H. I.; Grossfield, A.; MacKenzie, K. R.; Engelman, D. M.; Woolf, T. B. Modulation of glycophorin A transmembrane helix interactions by lipid bilayers: Molecular dynamics calculations. *J. Mol. Biol.* **2000**, *302* (3), 727−746.

(23) Bowie, J. U. Understanding membrane protein structure by design. *Nat. Struct. Biol.* **2000**, *7* (2), 91−94.

(24) Choma, C.; Gratkowski, H.; Lear, J. D.; DeGrado, W. F. Asparagine-mediated self-association of a model transmembrane helix. *Nat. Struct. Biol.* **2000**, *7* (2), 161−166.

(25) Zhou, F. X.; Cocco, M. J.; Russ, W. P.; Brunger, A. T.; Engelman, D. M. Interhelical hydrogen bonding drives strong interactions in membrane proteins. *Nat. Struct. Biol.* **2000**, *7* (2), 154−160.

(26) Zhou, F. X.; Merianos, H. J.; Brunger, A. T.; Engelman, D. M. Polar residues drive association of polyleucine transmembrane helices. *Proc. Natl. Acad. Sci. U.S.A.* **2001**, *98* (5), 2250−2255.

(27) Brown, M. F. Modulation of Rhodopsin Function by Properties of the Membrane Bilayer. *Chem. Phys. Lipids* **1994**, *73* (1−2), 159−180.

(28) Litman, B. J.; Mitchell, D. C. A role for phospholipid polyunsaturation in modulating membrane protein function. *Lipids* **1996**, *31*, S193-S197.

(29) Bezrukov, S. M.; Rand, R. P.; Vodyanoy, I.; Parsegian, V. A. Lipid packing stress and polypeptide aggregation: alamethicin channel probed by proton titration of lipid charge. *Faraday Discuss.* **1998**, *111*, 173−183.

(30) Greathouse, D. V.; Hinton, J. F.; Kim, K. S.; Koeppe, R. E. Gramicidin-a Short-Chain Phospholipid Dispersions − Chain-Length Dependence of Gramicidin Conformation and Lipid Organization. *Biochemistry-Us* **1994**, *33* (14), 4291−4299.

(31) Koeppe, R. E.; Andersen, O. S. Engineering the gramicidin channel. *Annu. Rev. Biophys. Biomol. Struct.* **1996**, *25*, 231−258.

(32) Fisher, L. E.; Engelman, D. M.; Sturgis, J. N. Detergents modulate dimerization but not helicity, of the glycophorin A transmembrane domain. *J. Mol. Biol.* **1999**, *293* (3), 639−651.

(33) Wang, W.; Donini, O.; Reyes, C. M.; Kollman, P. A. Biomolecular simulations: Recent developments in force fields, simulations of enzyme catalysis, protein−ligand, protein−protein, and protein-nucleic acid noncovalent interactions. *Annu. Rev. Biophys. Biomol. Struct.* **2001**, *30*, 211−243.

(34) Novotny, J.; Bruccoleri, R.; Karplus, M. An Analysis of Incorrectly Folded Protein Models − Implications for Structure Predictions. *J. Mol. Biol.* **1984**, *177* (4), 787−818.

(35) Bond, P. J.; Sansom, M. S. P. Membrane protein dynamics versus environment: Simulations of OmpA in a micelle and in a bilayer. *J. Mol. Biol.* **2003**, *329* (5), 1035−1053.

(36) Edholm, O.; Berger, O.; Jahnig, F. Structure and Fluctuations of Bacteriorhodopsin in the Purple Membrane − a Molecular-Dynamics Study. *J. Mol. Biol.* **1995**, *250* (1), 94−111.

(37) Crozier, P. S.; Stevens, M. J.; Forrest, L. R.; Woolf, T. B. Molecular dynamics simulation of dark-adapted rhodopsin in an explicit membrane bilayer: Coupling between local retinal and larger scale conformational change. *J. Mol. Biol.* **2003**, *333* (3), 493−514.

(38) Woolf, T. B.; Roux, B. Molecular-Dynamics Simulation of the Gramicidin Channel in a Phospholipid-Bilayer. *Proc. Natl. Acad. Sci. U.S.A.* **1994**, *91* (24), 11631−11635.

(39) Woolf, T. B.; Roux, B. Structure, energetics, and dynamics of lipid−protein interactions: A molecular dynamics study of the gramicidin A channel in a DMPC bilayer. *Proteins* **1996**, *24* (1), 92−114.

(40) Woolf, T. B.; Roux, B. The binding site of sodium in the gramicidin A channel: Comparison of molecular dynamics with solid-state NMR data. *Biophys. J.* **1997**, *72* (5), 1930−1945.

(41) Bond, P. J.; Faraldo-Gomez, J. D.; Sansom, M. S. P. OmpA: A pore or not a pore? Simulation and modeling studies. *Biophys. J.* **2002**, *83* (2), 763−775.

(42) Domene, C.; Sansom, M. S. P. Potassium channel, ions, and water: Simulation studies based on the high-resolution X-ray structure of KcsA. *Biophys. J.* **2003**, *85* (5), 2787−2800.

(43) Braun, R.; Engelman, D. M.; Schulten K. Molecular dynamics simulations of micelle formation around dimeric glycophorin A transmembrane helices. *Biophys. J.* **2004**, *87* (2), 754−763.

(44) Popot, J. L.; Engelman, D. M. Membrane-Protein Folding and Oligomerization − the 2-Stage Model. *Biochemistry-Us* **1990**, *29* (17), 4031−4037.

(45) Brooks, B. R.; Bruccoleri, R. E.; Olafson, B. D.; States, D. J.; Swaminathan, S.; Karplus, M. Charmm − a Program for Macromolecular Energy, Minimization, and Dynamics Calculations. *J. Comput. Chem.* **1983**, *4* (2), 187−217.

(46) Petrache, H. I.; Tristram-Nagle, S.; Nagle, J. F. Fluid phase structure of EPC and DMPC bilayers. *Chem. Phys. Lipids* **1998**, *95* (1), 83−94.

(47) Sagui, C.; Darden, T. A. Molecular dynamics simulations of biomolecules: Long-range electrostatic effects. *Annu. Rev. Biophys. Biomol. Struct.* **1999**, *28*, 155−179.

(48) Feller, S. E.; Pastor, R. W. Constant surface tension simulations of lipid bilayers: The sensitivity of surface areas and compressibilities. *J. Chem. Phys.* **1999**, *111* (3), 1281−1287.

(49) Vangunsteren, W. F.; Berendsen, H. J. C. Algorithms for Macromolecular Dynamics and Constraint Dynamics. *Mol Phys.* **1977**, *34* (5), 1311−1327.

(50) Volke, F.; Eisenblatter, S.; Galle, J.; Klose G. Dynamic Properties of Water at Phosphatidylcholine Lipid-Bilayer Surfaces as Seen by Deuterium and Pulsed-Field Gradient Proton Nmr. *Chem. Phys. Lipids* **1994**, *70* (2), 121−131.

(51) Aman, K.; Lindahl, E.; Edholm, O.; Hakansson, P.; Westlund, P. O. Structure and dynamics of interfacial water in an L-alpha phase lipid bilayer from molecular dynamics simulations. *Biophys. J.* **2003**, *84* (1), 102−115.

(52) Halle, B.; Wennerstrom, H. Interpretation of Magnetic-Resonance Data from Water Nuclei in Heterogeneous Systems. *J. Chem. Phys.* **1981**, *75* (4), 1928−1943.

(53) Arnold, K.; Pratsch, L.; Gawrisch K. Effect of Poly(Ethylene Glycol) on Phospholipid Hydration and Polarity of the External Phase. *Biochim. Biophys. Acta* **1983**, *728* (1), 121−128.

(54) Pratt, L. R.; Pohorille, A. Hydrophobic effects and modeling of biophysical aqueous solution interfaces. *Chem. Rev.* **2002**, *102* (8), 2671−2691.

(55) Gawrisch, K.; Ruston, D.; Zimmerberg, J.; Parsegian, V. A.; Rand, R. P.; Fuller, N. Membrane Dipole Potentials, Hydration Forces, and the Ordering of Water at Membrane Surfaces. *Biophys. J.* **1992**, *61* (5), 1213−1223.

(56) Sidhu, K. S.; Goodfellow, J. M.; Turner, J. Z. Effect of molecular shape and electrostatic interactions on the water layer around polar and apolar groups in solution. *J. Chem. Phys.* **1999**, *110* (16), 7943−7950.

(57) Creighton, T. E. *Proteins: Structures and Molecular Properties*; W. H. Freeman and Company: Heidelberg, 1996; 507 p.

(58) Wiener, M. C.; King, G. I.; White, S. H. Structure of a Fluid Dioleoylphosphatidylcholine Bilayer Determined by Joint Refinement of X-ray and Neutron-Diffraction Data. 1. Scaling of Neutron Data and the Distributions of Double-Bonds and Water. *Biophys. J.* **1991**, *60* (3), 568−576.

(59) Wiener, M. C.; White, S. H. Structure of a Fluid Dioleoylphosphatidylcholine Bilayer Determined by Joint Refinement of X-ray and Neutron-Diffraction Data. 2. Distribution and Packing of Terminal Methyl-Groups. *Biophys. J.* **1992**, *61* (2), 428−433.

(60) Wiener, M. C.; White, S. H. Structure of a Fluid Dioleoylphosphatidylcholine Bilayer Determined by Joint Refinement of X-ray and Neutron-Diffraction Data. 3. Complete Structure. *Biophys. J.* **1992**, *61* (2), 434−447.

(61) Nagle, J. F.; Tristram-Nagle, S. Structure of lipid bilayers. *BBA-Rev Biomembranes* **2000**, *1469* (3), 159−195.

(62) Nagle, J. F.; Tristram-Nagle, S. Lipid bilayer structure. *Curr. Opin. Struct. Biol.* **2000**, *10* (4), 474−480.

(63) Fodje, M. N.; Al-Karadaghi, S. Occurrence, conformational features and amino acid propensities for the pi-helix. *Protein Eng.* **2002**, *15* (5), 353−358.

(64) Chakrabartty, A.; Schellman, J. A.; Baldwin, R. L. Large Differences in the Helix Propensities of Alanine and Glycine. *Nature* **1991**, *351* (6327), 586−588.

(65) Tieleman, D. P.; Sansom, M. S. P.; Berendsen, H. J. C. Alamethicin helices in a bilayer and in solution: Molecular dynamics simulations. *Biophys. J.* **1999**, *76* (1), 40−49.

(66) Tieleman, D. P.; Woolley, G. A.; Sansom, M. S. P. Alamethicin as model system for ion selectivity: Computational studies. *Biophys. J.* **2000**, *78* (1), 174a-174a.

(67) Korzhnev, D. M.; Orekhov, V. Y.; Arseniev, A. S.; Gratias, R.; Kessler, H. Mechanism of the unfolding of transmembrane alpha-helical segment (1−36)-bacteriorhodopsin studied by molecular dynamics simulations. *J. Phys. Chem. B* **1999**, *103* (33), 7036−7043.

(68) Marqusee, S.; Robbins, V. H.; Baldwin, R. L. Unusually Stable Helix Formation in Short Alanine-Based Peptides. *Proc. Natl. Acad. Sci. U.S.A.* **1989**, *86* (14), 5286−5290.

(69) Scholtz, J. M.; York, E. J.; Stewart, J. M.; Baldwin, R. L. A Neutral, Water-Soluble, Alpha-Helical Peptide − the Effect of Ionic-Strength on the Helix Coil Equilibrium. *J. Am. Chem. Soc.* **1991**, *113* (13), 5102−5104.

(70) Vila, J. A.; Ripoll, D. R.; Scheraga, H. A. Physical reasons for the unusual alpha-helix stabilization afforded by charged or neutral polar residues in alanine-rich peptides. *Proc. Natl. Acad. Sci. U.S.A.* **2000**, *97* (24), 13075−13079.

(71) Nilsson, I.; Johnson, A. E.; von Heijne, G. How hydrophobic is alanine? *J. Biol. Chem.* **2003**, *278* (32), 29389−29393.

(72) Cheng, J. X.; Pautot, S.; Weitz, D. A.; Xie, X. S. Ordering of water molecules between phospholipid bilayers visualized by coherent anti-Stokes Raman scattering microscopy. *Proc. Natl. Acad. Sci. U.S.A.* **2003**, *100* (17), 9826−9830.

(73) Gawrisch, K.; Richter, W.; Mops, A.; Balgavy, P.; Arnold, K.; Klose, G. The Influence of Water Concentration on the Structure of Egg-Yolk Phospholipid Water Dispersions. *Stud. Biophys.* **1985**, *108* (1), 5-16.

(74) Petrache, H. I.; Tristram-Nagle, S.; Gawrisch, K.; Harries, D.; Parsegian, V. A.; Nagle, J. F. Structure and fluctuations of charged phosphatidylserine bilayers in the absence of salt. *Biophys. J.* **2004**, *86* (3), 1574−1586.

(75) Ho, C.; Stubbs, C. D. Hydration at the Membrane Protein−Lipid Interface. *Biophys. J.* **1992**, *63* (4), 897−902.

(76) Wang, H. B.; Carlson, E.; Henderson, D.; Rowley, R. L. Molecular dynamics simulation of the liquid−liquid interface for immiscible and partially miscible mixtures. *Mol. Simulat.* **2003**, *29* (12), 777−785.

(77) Tikhonov, A. M.; Schlossman, M. L. Surfactant and water ordering in triacontanol monolayers at the water-hexane interface. *J. Phys. Chem. B* **2003**, *107* (15), 3344−3347.

CT049928Y